



# Impact of partial volume effect correction on cerebral $\beta$ -amyloid imaging in APP-Swe mice using [ $^{18}\text{F}$ ]-florbetaben PET<sup>☆</sup>

Matthias Brendel<sup>a</sup>, Andreas Delker<sup>a</sup>, Christina Rötzer<sup>a</sup>, Guido Böning<sup>a</sup>, Janette Carlsen<sup>a</sup>, Clemens Cyran<sup>b</sup>, Erik Mille<sup>a</sup>, Franz Josef Gildehaus<sup>a</sup>, Paul Cumming<sup>c</sup>, Karlheinz Baumann<sup>d</sup>, Harald Steiner<sup>f,g</sup>, Christian Haass<sup>e,f,g</sup>, Jochen Herms<sup>e,f,h</sup>, Peter Bartenstein<sup>a,e</sup>, Axel Rominger<sup>a,\*</sup>

<sup>a</sup> Department of Nuclear Medicine, Ludwig-Maximilians-University, Munich, Germany

<sup>b</sup> Department of Clinical Radiology, Ludwig-Maximilians-University, Munich, Germany

<sup>c</sup> Department of Nuclear Medicine, University of Erlangen/Nuremberg, Germany

<sup>d</sup> F. Hoffmann-La Roche, Basel, Switzerland

<sup>e</sup> Munich Cluster for Systems Neurology (SyNergy), Munich, Germany

<sup>f</sup> German Center for Neurodegenerative Diseases (DZNE), Ludwig-Maximilians-University, Munich, Germany

<sup>g</sup> Adolf-Butenandt-Institute, Biochemistry, Ludwig-Maximilians-University, Munich, Germany

<sup>h</sup> German Center for Neurodegenerative Diseases (DZNE) - Department for Translational Brain Research, Ludwig-Maximilians-University, Munich, Germany

## ARTICLE INFO

### Article history:

Accepted 10 September 2013

Available online 20 September 2013

### Keywords:

Partial volume effect correction

Small animal PET

Alzheimer's disease

$\beta$ -amyloid

[ $^{18}\text{F}$ ]-florbetaben

## ABSTRACT

We previously investigated the progression of  $\beta$ -amyloid deposition in brain of mice over-expressing amyloid-precursor protein (APP-Swe), a model of Alzheimer's disease (AD), in a longitudinal PET study with the novel  $\beta$ -amyloid tracer [ $^{18}\text{F}$ ]-florbetaben. There were certain discrepancies between PET and autoradiographic findings, which seemed to arise from partial volume effects (PVE). Since this phenomenon can lead to bias, most especially in the quantitation of brain microPET studies of mice, we aimed in the present study to investigate the magnitude of PVE on [ $^{18}\text{F}$ ]-florbetaben quantitation in murine brain, and to establish and validate a useful correction method (PVEC). Phantom studies with solutions of known radioactivity concentration were performed to measure the full-width-at-half-maximum (FWHM) resolution of the Siemens Inveon DPET and to validate a volume-of-interest (VOI)-based PVEC algorithm. Several VOI-brain-masks were applied to perform in vivo PVEC on [ $^{18}\text{F}$ ]-florbetaben data from C57BL/6(N = 6) mice, while uncorrected and PVE-corrected data were cross-validated with gamma counting and autoradiography. Next, PVEC was performed on longitudinal PET data set consisting of 43 PET scans in APP-Swe (13–20 months) and age-matched wild-type (WT) mice using the previously defined masks. VOI-based cortex-to-cerebellum ratios (SUVR) were compared for uncorrected and PVE-corrected results. Brains from a subset of transgenic mice were ultimately examined by autoradiography ex vivo and histochemistry in vitro as gold standard assessments, and compared to VOI-based PET results.

The phantom study indicated a FWHM of 1.72 mm. Applying a VOI-brain-mask including extracerebral regions gave robust PVEC, with increased precision of the SUVR results. Cortical SUVR increased with age in APP-Swe mice compared to baseline measurements (16 months: +5.5%,  $p < 0.005$ ; 20 months: +15.5%,  $p < 0.05$ ) with uncorrected data, and to a substantially greater extent with PVEC (16 months: +12.2%  $p < 0.005$ ; 20 months: +36.4%  $p < 0.05$ ). WT animals showed no binding changes, irrespective of PVEC. Relative to autoradiographic results, the error [%] for uncorrected cortical SUVR was 18.9% for native PET data, and declined to 4.8% upon PVEC, in high correlation with histochemistry results. We calculate that PVEC increases by 10% statistical power for detecting altered [ $^{18}\text{F}$ ]-florbetaben uptake in aging APP-Swe mice in planned studies of disease modifying treatments on amyloidogenesis.

© 2013 Elsevier Inc. All rights reserved.

**Abbreviations:** APP-Swe, K670N; M671L, mutation of amyloid precursor protein; BAS, basal surround VOI; BGR, background surround VOI; CBL, cerebellum; CTX, cortex; ET, effects of therapy; FoV, Field of View; FWHM, full width at half maximum; FRO, frontal surround VOI; GTM, geometric transfer matrix; HGL, harderian gland VOI; HIP, hippocampus; PVE, partial volume effects; MGM, Müller-Gärtner Method; MIX, combined brain structure VOI except frontal cortical target VOI and cerebellum; MIX-HI, high uptake part of subdivided MIX VOI; MIX-LO, low uptake part of subdivided MIX VOI; PSF, point spread function; PVEC, partial volume effect correction; RMSE [%], root-mean-square-error percentage; SPI, spinal surround VOI; SRR, single extracerebral surround VOI; SUP, superior surround VOI; TG, transgenic; WT, wild-type.

<sup>☆</sup> Financial support: The study was supported by the SyNergy Cluster.

\* Corresponding author. Fax: +49 89 7095 7646.

E-mail address: [axel.rominger@med.uni-muenchen.de](mailto:axel.rominger@med.uni-muenchen.de) (A. Rominger).

## Introduction

Alzheimer's disease (AD) is imposing a growing socioeconomic burden due to the aging population demographics, especially in industrialized nations (Ziegler-Graham et al., 2008). Present treatments are symptomatic, but some promising avenues for disease-modifying treatment are in different phases of development and approval (Singh et al., 2012). In general animal models represent an important tool for pre-clinical testing of disease progression and novel medications in conjunction with molecular imaging (Virdee et al., 2012). A number of rodent AD-models are characterized by cerebral overexpression of  $\beta$ -amyloid and progressive formation of cortical  $\beta$ -plaques, emulating this aspect of AD pathology (Teipel et al., 2011). The prospect of monitoring disease progression in individual animals has given rise to a number of rodent positron emission tomography (PET) studies in conjunction with [ $^{11}\text{C}$ ]- or [ $^{18}\text{F}$ ]-labeled  $\beta$ -amyloid-tracers (Klunk et al., 2005; Maeda et al., 2007; Manook et al., 2012; Poisnel et al., 2012; Rojas et al., 2013; Snellman et al., 2012; Toyama et al., 2005). Quantitative analysis of PET data from rodent brain is necessarily compromised by partial volume effects (PVE), which result in degradation of signals from target sources of the same scale as the spatial resolution of the tomograph (Kuntner et al., 2009). However, there have been few reports of small animal PET-PVE, despite its great significance for PET quantification (Erlandsson et al., 2012). In the majority of previous human studies, PVE correction (PVEC) of brain signals has been based on the Müller-Gärtner Method (MGM) and its modifications (Thomas et al., 2011) which depend on voxel-based geometric transfer matrix (GTM) models first established by Videen and coworkers (Videen et al., 1988).

We previously investigated the progression of  $\beta$ -amyloid deposition in brain of AD-model mice over-expressing a human mutation of the amyloid-precursor protein (APP-Swe), in a longitudinal PET study with the novel  $\beta$ -amyloid tracer [ $^{18}\text{F}$ ]-florbetaben (Rominger et al., 2013). We reported a notable increase in  $\beta$ -amyloid PET signal from the brain of APP-Swe mice with age, which significantly correlated with histochemical findings post mortem. However, there were also distinct discrepancies between cortex-to-cerebellum standard uptake value ratios (SUVR) measured by PET in vivo and the more pronounced accumulation measured ex vivo. Similar discrepancies have been described in a study with the alternate  $\beta$ -amyloid tracer [ $^{18}\text{F}$ ]-AV-45 (Poisnel et al., 2012), and are likely attributable to PVE.

With this background, we aimed to establish the magnitude of PVE on quantitation of  $\beta$ -amyloid burden in the mouse brain with [ $^{18}\text{F}$ ]-florbetaben, and to implement and validate PVEC for our AD mouse model. We predicted that PVE-correction of PET recordings should enhance the precision of the method, this affording more sensitive detection of planned disease-modifying treatments and to reductions in required sample sizes.

## Materials and methods

### Phantom studies

#### Estimation of spatial resolution

Indwelling venous cannulae (Vasofix® Safety; B. Braun Melsungen AG, Germany) of three different internal diameters (0.4, 0.6 and 0.8 mm) were cut into 20 mm lengths, filled with a solution containing eosin and [ $^{18}\text{F}$ ] (61.56 MBq/cc), and sealed at both ends with superglue. Two sources of each diameter were placed in a cylindrical phantom chamber (volume 41.2 ml), and held in place with modeling clay at an interval of 8 mm (Fig. 1A). The phantom chamber was then filled with water containing [ $^{18}\text{F}$ ] (0.07 MBq/cc), i.e. background activity approximately 0.1% of the target activity concentration. The phantom was then placed in the aperture of the Siemens Inveon DPET, with the tubular sources in horizontal orientation. The acquisition protocol consisted of a 60 min emission scan, followed by a 15 min transmission scan using a rotating [ $^{57}\text{Co}$ ] point source, resulting in a single frame

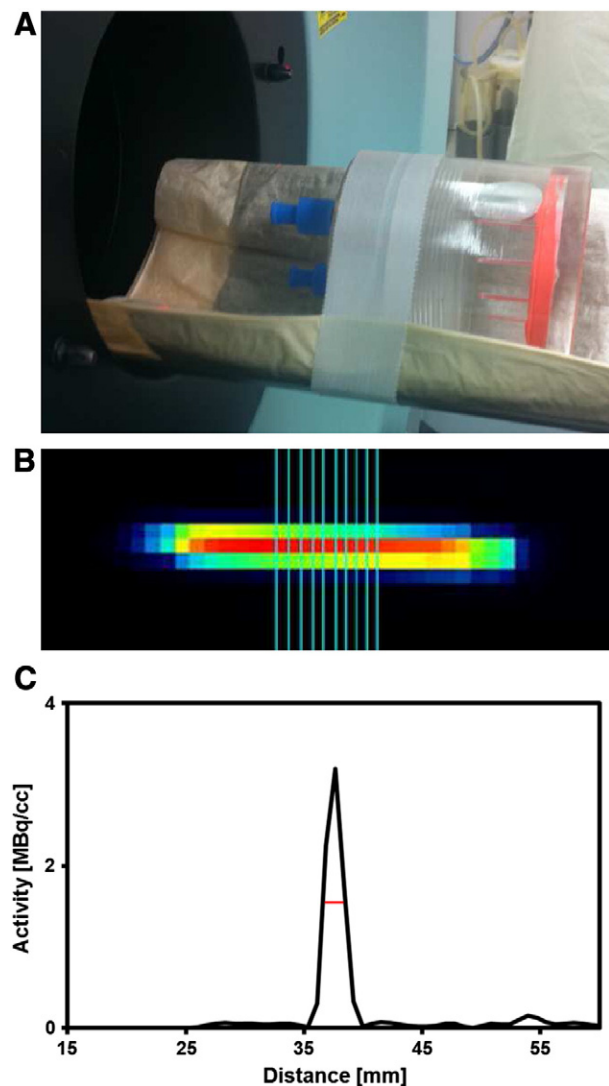


**Fig. 1.** (A) [ $^{18}\text{F}$ ]-filled cylindric phantom in transaxial position in front of the aperture of the small animal PET scanner. Cannulae appear red due to filling with eosin marker solution and contain [ $^{18}\text{F}$ ] at a range of radioactivity concentrations. They are fixed in transaxial position with modeling clay (orange) within the phantom. (B) Corresponding PET scan of a [ $^{18}\text{F}$ ]-filled single cannula (inner diameter 0.8 mm) immersed in an [ $^{18}\text{F}$ ]-background of 1000-fold less activity concentration. Voxel dimensions are  $0.78 \times 0.78 \times 0.80$  mm, i.e. oversampled relative to the FWHM. Blue lines in axial direction show applied line profiles. (C) Resulting line profile as a function of distance for averaged 120 line profiles in the horizontal axial direction. Red line indicates the mean FWHM value (1.72 mm) arising from this calculation.

(3600 s). A second acquisition was acquired after rotating the phantom by  $90^\circ$ , placing the tubular sources in a vertical orientation. As described in detail previously, (Rominger et al., 2013) the reconstruction consisted of 4 OSEM3D and 32 MAP3D iterations, a zoom of 1.0, with scatter and decay correction, resulting in a final  $128 \times 128 \times 159$  matrix of voxels measuring  $0.78 \times 0.78 \times 0.80$  mm. The reconstruction algorithm as implemented by the tomograph's manufacturer accounts for the space-variant detector response and yields a high and nearly space-invariant spatial resolution (Qi and Leahy, 2000; Visser et al., 2009). Due to the improved resolution properties of this algorithm it provides substantially enhanced quantitative accuracy compared to standard filtered back projection, even in case of low count statistics in dynamic PET measurements (Cheng et al., 2012).

Line profiles were generated within Amide image analyzing software (V0.8.22; <http://amide.sourceforge.net>) in ten consecutive voxel-layers through the midline of each cannula in the X and Y

Download English Version:

<https://daneshyari.com/en/article/6028607>

Download Persian Version:

<https://daneshyari.com/article/6028607>

[Daneshyari.com](https://daneshyari.com)